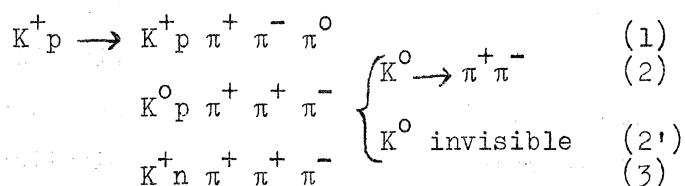


EVIDENCE FOR  $K(725)$  IN  $K^+p$  INTERACTIONS AT 3 GEV/C

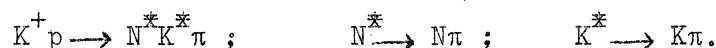
M. Ferro-Luzzi, R. George, Y. Goldschmidt-Clermont, V.P. Henri, B. Jongejans,  
D.W.G. Leith, G.R. Lynch, F. Muller and J.-M. Perreau,

CERN - - Geneva

In a 3.0 GeV/c  $K^+$  exposure of the 81 cm Saclay hydrogen bubble chamber at the CERN proton synchrotron, the following reactions have been studied :



The cross-sections for these reactions are about 0.8 mb for (1), 0.4 mb for (2) plus (2'), and 0.2 mb for (3). The analysis of the above channels shows that the reactions proceed mainly via production of  $N^*(1238)$  in conjunction with  $K^*(890)$ , viz. :



In addition, we observe the production of  $\omega^0$  with a cross-section of about 100 $\mu$ b in reaction (1).

In all the reactions (1) - (3), we have also evidence for the production of  $K$  in the two charge states,  $K^+$  and  $K^0$ . The cross-section for production of  $K^+$  and  $K^0$  in these reactions is about 80 $\mu$ b and 60 $\mu$ b, respectively. It should be noticed that no indication for  $K$  production has been found in 3 and 4-body reactions of  $K^+p$  at the same energy<sup>1,2</sup>). (The limit for the cross-sections for  $K^+$  and  $K^0$  production from the latter reactions is  $(0 \pm 20)$   $\mu$ b.) We find a value of  $M = (725 \pm 5)$  Mev and  $\Gamma < 30$  Mev for the mass and width of the  $K$ .

The above reactions have been found among the 4-prong and 4-prong plus  $V^0$  topologies. Different fiducial volumes in the bubble chamber have been used for the two topologies, yielding a total of 312 events of reaction (1), 113 of reaction (2) with a visible  $K^0$  decay, 123 of reaction (2) with no visible  $K^0$  decay, and 71 events of reaction (3). These events were processed through the standard CERN analysis programmes. Each event was examined on the scanning table for

compatibility of ionisation with the results of the fitting programme.

The events from reaction (2') have not been used for detailed analysis and will be presented only to demonstrate their consistency with those from reaction (2); the reason for this being that the mass resolution for two-body combinations in reaction (2') is from 2 to 3 times worse than in the corresponding reaction where the  $K^0$  decay is seen.

In Fig. 1 the mass distributions of the  $(\pi^+p)$  system for reactions (1) and (2), and of the  $(\pi^-n)$  systems from reaction (3), are presented. The solid curve is the sum of a Breit-Wigner resonance shape for the  $N_{3,3}^*$  (shown independently as a dotted line), and a five-body phase space distribution; the two contributions are about equal. Also shown in the figure, as the shaded areas, are the  $p\pi^+$  spectra where one of the remaining  $I_Z = 1/2$  ( $K\pi$ ) combinations has a mass corresponding to the  $K^*(890)$ . That is, for Fig. 1a, the mass of the  $(K^+\pi^0)$  or  $(K^+\pi^-)$  combinations must lie between  $(0.86 - 0.94)$  GeV, and for Fig. 1b, the mass of the  $K^0$ , together with one of the  $\pi^+$ , should lie within  $(0.86 - 0.94)$  GeV, when the mass of the combination of the proton and the other  $\pi^+$  is taken. These sub-spectra show a good fit to the Breit-Wigner distribution for the  $N^*$  (the dotted curves), and since these dotted curves were independently normalised using the total data, the shaded areas indicate that practically all the  $N_{3,3}^*$ 's are produced together with a  $K^*(890)$ . Such a situation is not possible, of course, for reaction (3) where the  $\pi^-$  is common.

In Figs. 2 and 3 the  $T_Z = 1/2$  ( $K\pi$ ) spectra are shown. The  $(K^+\pi^0)$  in (2a), and  $(K^+\pi^-)$  in (2b) belong to reaction (1), while the  $(K^0\pi^+)$  in (2c) comes from reaction (2). The full lines on these plots are attempts to fit the data using only a Breit-Wigner resonance shape for the  $K^*$ , and a five-body phase space distribution for the background. The shaded region on these plots corresponds to events in which the  $p\pi^+$  mass is inside the  $N_{3,3}^*$  (i.e.  $1.16 \leq M(p\pi^+) \leq 1.29$  GeV). (The  $K^0\pi^+$  combination, in Fig. 2c, is shaded where the  $(P + \text{other } \pi^+)$  combination has a mass within the given range.) The dotted curve is a fitting to the shaded area, excluding the  $K^*$  region, and using a four-body phase space distribution corresponding to a  $(N^*K\pi\pi)$  final state. It may be seen that in the spectrum of Fig. 2c, the width of the  $K^*(890)$  and of the enhancement at 725 Mev are much smaller than those for reaction (1), due to the improved resolution for those events where all five particles are

seen. In Fig. 3a and 3b the  $(K^0\pi^+)$  mass spectrum from reaction (2') and  $(K^+\pi^-)$  from reaction (3) are respectively displayed. The same general features characterising the spectra of Fig. 2 can be observed here, providing confirmation for the better resolution channels. From these spectra it may be concluded that, in addition to the production of  $K^*$  there is evidence for the production of a  $(K\pi)$  system of mass around 725 Mev, in all three channels and in both charge states. We shall now identify this enhancement with the  $K(725)$  meson<sup>3,4</sup>. It may be further pointed out that the  $K(725)$  does not appear to be produced predominantly in conjunction with the  $N_{3,3}^*$ .

The  $T = 3/2$   $(K\pi)$  combinations are plotted in Fig. 4, where the  $(K^+\pi^+)$  spectrum from reaction (1) is shown in (a), and the  $(K^0\pi^-)$  spectrum from reaction (2) is shown in (b). The curves shown are modified phase space distributions taking into account the production of  $N^*$  in these reactions. The fits to the data are reasonably good, in agreement with the expectation for the case of a  $K^*$  and  $K$  of I-spin = 1/2. Furthermore, these plots show that it is reasonable to assume that the presence of a "wrong"  $(K\pi)$  combination when two possible  $K^*$  can be made, contributes to the overall plot simply as a background ("phase space") event. In this connection it should be noticed that reactions (1) also show production of  $\omega^0 \rightarrow \pi^+\pi^-\pi^0$  in about 15% of the cases. The  $\omega^0$  peak clearly stands up over a background of about the same magnitude. Rather than eliminating both the  $\omega$ -events and the "background" ones, we have verified that these events are distributed in a phase-space-like manner when  $K\pi$  and  $p\pi$  combinations are formed.

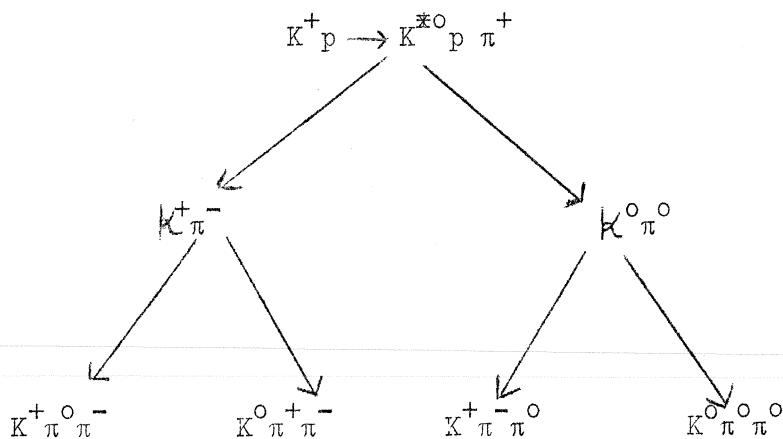
Fig. 5a presents the overall  $(K^+\pi^0)$ ,  $(K^+\pi^-)$  and  $(K^0\pi^+)$  mass spectrum from reactions (1) and (2) (each event has two entries in the plot). The curve is, once more, a fitting to the data assuming only a five-body phase space distribution and a Breit-Wigner resonance form for the  $K^*(890)$ . The fit is good everywhere except in the  $(K\pi)$  mass region around (700 - 750) Mev, where there is an excess of events of  $\sim 3$  standard deviations significance which can be attributed to the formation of  $K(725)$ . The production cross-section for  $K^+$  in the reactions (1), (2) and (2') is about 45 $\mu$ b, and 40 $\mu$ b, respectively, and for  $K^0$  in reactions (1) and (3), it is about 40 $\mu$ b and 25 $\mu$ b, respectively. Inspection of Fig. 5a shows that the enhancement is centred around 725 Mev, and has an

experimental width at half height of about 30 Mev. Allowing for the experimental resolution in the region of the peak, we can set a lower limit to the real  $\kappa$  width of  $\sim 20$  Mev, but have to point out that there are broadenings, or fluctuations, in Fig. 2 for the  $K^*$  as well as the  $\kappa$ , which are only partly explained by our resolution.

In Fig. 5b, we have subtracted out the 'non-resonant'  $K\pi\pi N^*$  background, using the fit obtained in Fig. 2 (dotted lines). This subtraction should then leave the resonant ( $K\pi$ ) events together with the non-resonant events distributed according to simple five-body phase space. It may be seen from the figure that the magnitude of the enhancement at 725 Mev has remained essentially intact, emphasizing the fact that this resonance is not produced in conjunction with  $N_{3,3}^*$ . A study of the other possible resonances (i.e.  $\pi\text{-}\pi$ ,  $p\text{-}\pi$ ,  $p\pi\pi$  states), which may be produced in association with the kappa yielded a negative result.

Having established the presence of  $\kappa(725)$  in our reactions, we now discuss its decay ratios. Table I gives the expected and observed branching ratios for  $\kappa$  decay into  $K^+\pi^0$  and  $K^0\pi^+$ : analogous data for the  $K^*$  decay are also presented for comparison. The data are in good agreement with isospin  $1/2$  for both resonances, thus confirming the indication against  $I = 3/2$  for the derived from Fig. 4.

The decay of the  $K^* \rightarrow \kappa + \pi$  is energetically possible and may be used to throw some light on the spin-parity of the  $\kappa$ . The allowed spin-parity assignments for the kappa are  $0^+$ ,  $1^-$ ,  $2^+$ , etc., but in the event of a  $K^* \rightarrow \kappa\pi$  decay mode being observed, the  $0^+$  assignment would be forbidden. If the  $\kappa$ 's observed in the reactions (1) and (2) come from  $K^*$  decay, then one might expect them to be derived from the following chain :



The normal decay mode of the parent  $K^*$  would then be found in the following reactions :



The study of these latter reactions is reported elsewhere<sup>2)</sup>. Here we can use the total number of  $K^*$ 's (890) found in reactions (4) and (5), where no  $N_{3,3}^*$  is present, together with an examination of the  $K\pi$  mass distribution in reactions (1) and (2) to obtain a decay ratio. We use only the number of  $K^*$  produced without an associated  $N_{3,3}^*$ , since the kappa does not appear to be produced together with  $N_{3,3}^*$ . The fraction of  $K^* N\pi$  events is  $\sim 5\%$  for reaction (4), and  $\sim 7\%$  for reaction (5). The decay ratio thus found is

$$\frac{K^* \rightarrow K + \pi}{K^* \rightarrow K + \pi} < 0.01.$$

The expected branching ratio would <sup>be</sup> 0 for  $0^+$  spin-parity  $K$ , and is difficult to calculate for higher spins. However, Glashow has estimated the branching ratio for the  $1^-$  assignment, using  $SU_3$  symmetry, and obtains a value of 0.06. The data may therefore be taken as an indication for  $0^+$  spin-parity for the kappa meson.

The centre of mass production angular distribution for the  $K$  is indistinguishable from that of the background, which is consistent with isotropy. This is in contrast with the  $K^*$  events, which show prominent forward emission.

#### ACKNOWLEDGMENTS

We would like to thank the P.S. staff and the crew of the Saclay bubble chamber team for their invaluable help throughout the experiment, and the IEP and computer groups and our scanning teams for their part in the analysis. We are grateful to Dr. R. Armenteros and to Professor Ch. Peyrou for their interest and support.

REFERENCES

- 1) M. Ferro-Luzzi, R. George, Y. Goldschmidt-Clermont, V.P. Henri, B. Jongejans, D.W.G. Leith, G.R. Lynch, F. Muller and J.-M. Perreau, Proceedings of the Sienna International Conference on Elementary Particles, Vol.1, 189 (1963), and "The Reaction  $K^+ p \rightarrow K^0 p \pi^+$  at 3 GeV/c", submitted to Physical Review.  
G.R. Lynch, M. Ferro-Luzzi, R. George, Y. Goldschmidt-Clermont, V.P. Henri, B. Jongejans, D.W.G. Leith, F. Muller and J.-M. Perreau, Physics Letters 9, 359 (1964).
- 2) M. Ferro-Luzzi, R. George, Y. Goldschmidt-Clermont, V.P. Henri, B. Jongejans, D.W.G. Leith, G.R. Lynch, F. Muller and J.-M. Perreau, "Four-body final states in 3 GeV/c  $K^+ p$  interactions", to be submitted to Physical Review.
- 3) D.H. Miller, G. Alexander, O. Dahl, L. Jacobs, G.R. Kalbfleisch and G.A. Smith, Physics Letters 5, 279 (1963).
- 4) S.G. Wojcicki, G.R. Kalbfleisch and M.H. Alston, Physics Letters 5, 283 (1963).  
P.L. Connolly, E.L. Hart, G. Kalbfleisch, K.W. Lai, G. London, G.C. Moneti, R.R. Rau, N.P. Samios, I.O. Skillicorn, S.S. Yamamoto, M. Goldberg, M. Gundzik, J. Leitner and S. Lichtman, Proceedings of the Sienna International Conference on Elementary Particles, Vol. 1, 125 (1963).
- 5) S.L. Glashow, Athens Conference on Recently Discovered Resonant Particles, 1963.

FIGURE CAPTIONS

- Fig. 1 a) The  $(p\pi^+)$  mass spectra from reaction (1), and b), from reaction (2).  
 c) The  $(n\pi^-)$  spectrum from reaction (3). The plots contain 312 events, 113 x 2 events and 71 events, respectively. The solid line is a fitting to the data with a P-wave Breit-Wigner resonance shape for the  $N^*$  (shown separately as dotted), and a 5-body phase space distribution for the background. The fits are for equal amounts of resonance and background. The shaded area represents those events in which there is also a  $(K\pi)$  combination to be associated with the  $K^*(890)$ .
- Fig. 2 The  $(K^+\pi^0)$  and  $(K^+\pi^-)$  mass spectra, from reaction (1) - a), b) - respectively. (each histogram contains 312 events), and the  $(K^0\pi^+)$  spectrum from reaction (2) - c) (113 x 2 events). The full line curves are the fits to the data using a P-wave Breit-Wigner shape for the  $K^*$ , with  $M = 890$  Mev and  $\Gamma = 50$  Mev, and 5-body phase space distribution for the background. The shaded area corresponds to events which have a  $(p\pi^+)$  combination with mass associated with  $N_{3,3}^*$ . The dotted line is a fitting of a modified phase space distribution to the events produced with  $N_{3,3}^*$ , but neglecting the region of the  $K^*$ .
- Fig. 3 a) The  $(K^0\pi^+)$  mass spectrum from reaction (2') (123 x 2 events), and b) the  $(K^+\pi^-)$  spectrum from reaction (3) (71 events).
- Fig. 4 a) The  $(K^+\pi^+)$  mass spectrum from reaction (1) (312 events), and b) the  $(K^0\pi^-)$  spectrum from reaction (2) (113 events). The full line curves are modified phase space distribution, taking into account the production of  $N_{3,3}^*$ .
- Fig. 5 a) The sum of the  $(K^+\pi^-)$  and  $(K^+\pi^0)$  spectra from reaction (1) and the  $(K^0\pi^+)$  spectra from reaction (2) (425 x 2 events). The solid curve is a fitting to the data with a P-wave Breit-Wigner shape from the  $K^*(890)$ , width of 50 Mev, and a 5-body phase space distribution for the background.  
 b) The overall  $(K\pi)_{I=1/2}$  spectrum as in Fig. 5a), with those events produced with an  $N_{3,3}^*$  subtracted out.

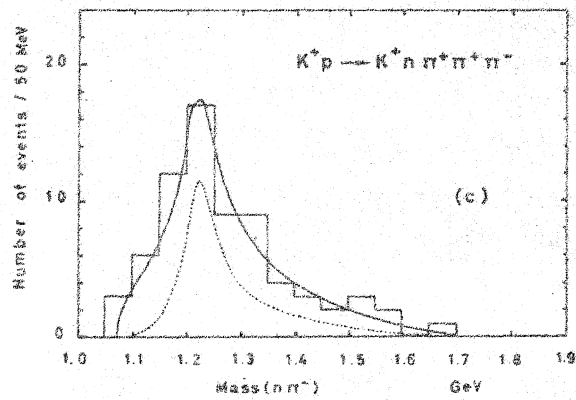
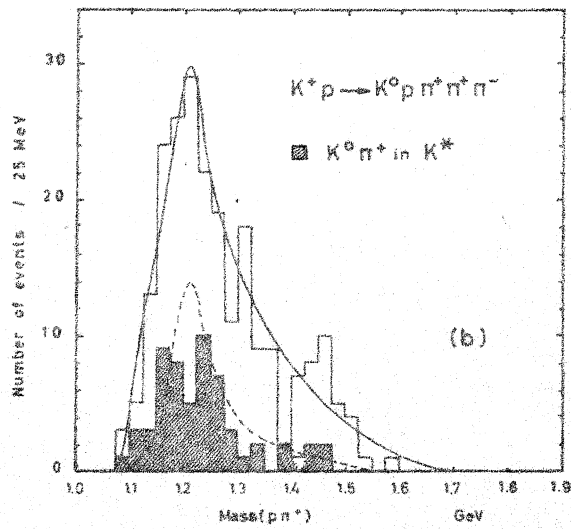
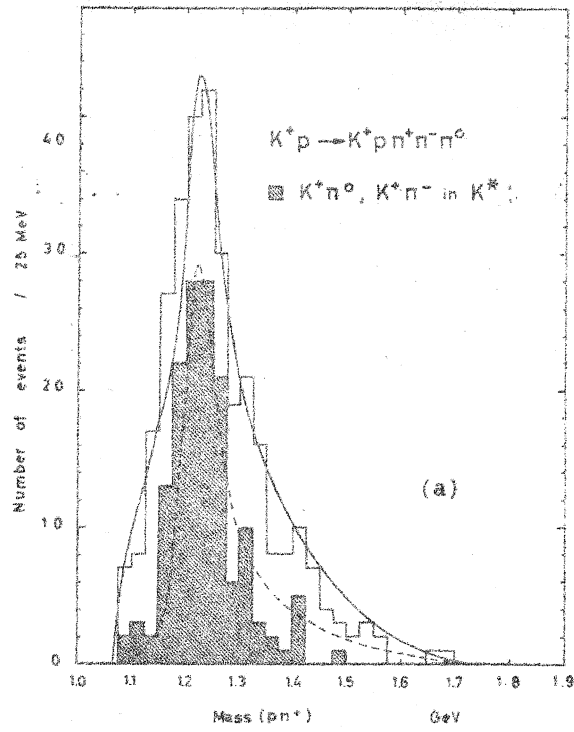
TABLE I

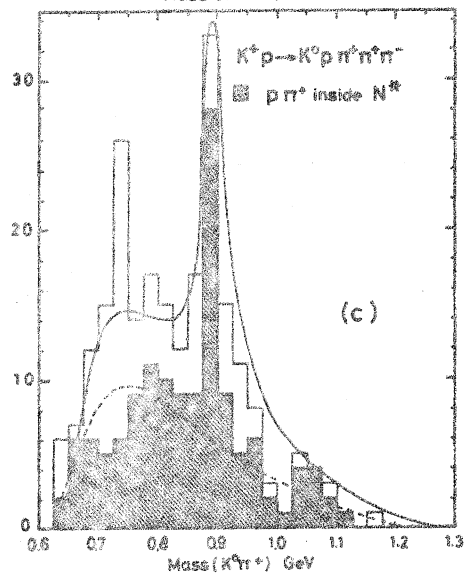
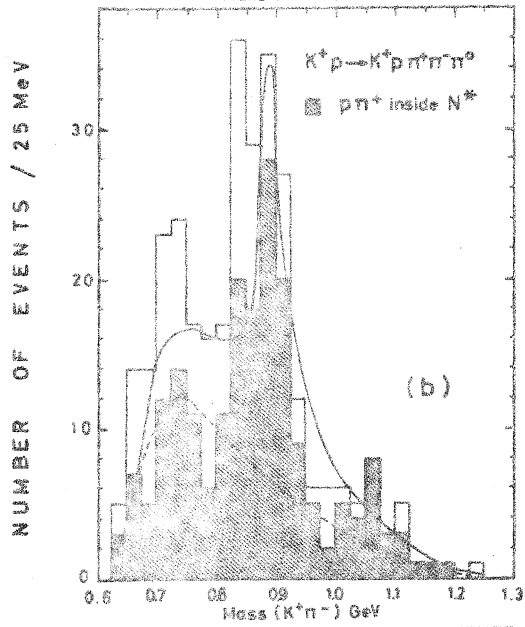
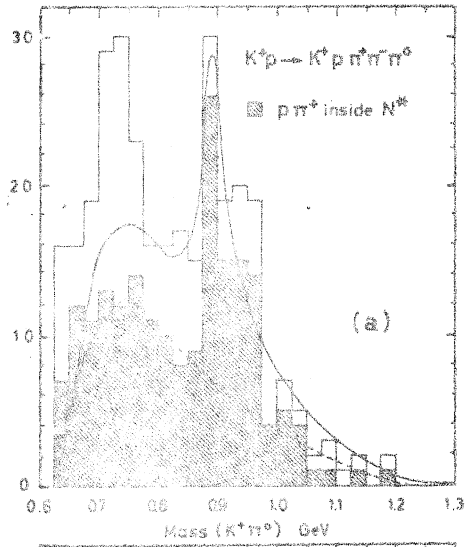
 $K^*(890)$  and  $K(725)$  Branching Ratios

State	$K^*(890)$	$K(725)$
$K^0 \pi^+$ (from reaction (2))	$69 \pm 10^a$	$28 \pm 8^a$
$K^+ \pi^0$ (from reaction (1))	$45 \pm 8$	$20 \pm 7$
Branching Ratio Observed	$1.5 \pm 0.4$	$1.4 \pm 0.8$
Expected Branching Ratio for $I = 1/2$	2.0	
Expected Branching Ratio for $I = 3/2$	0.5	

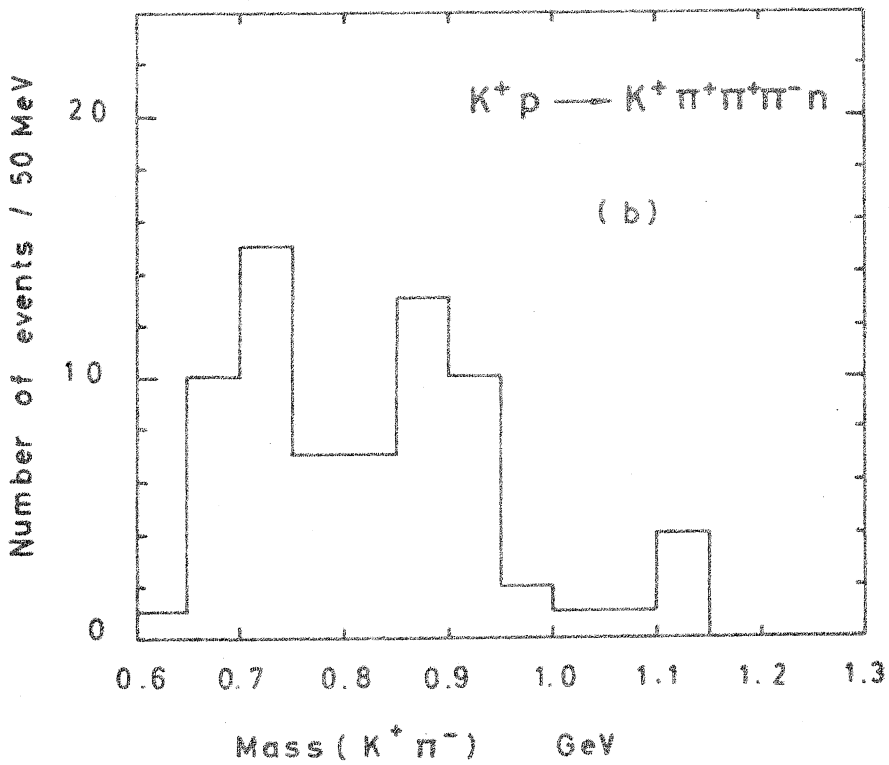
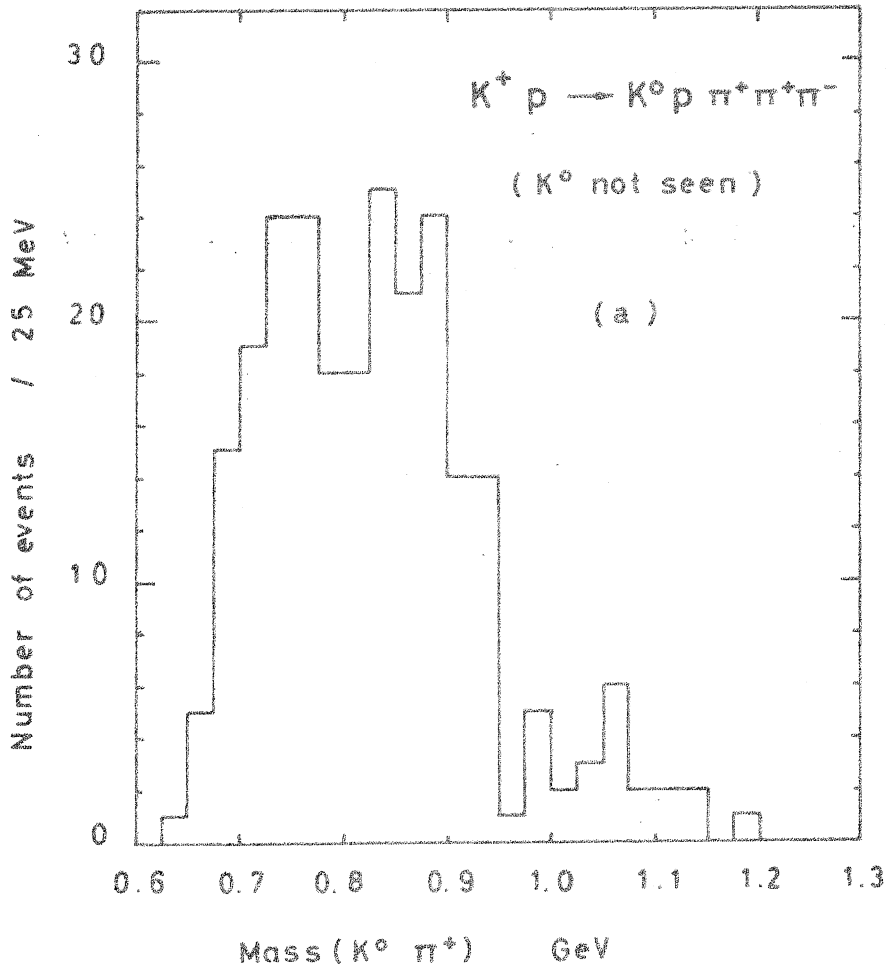
a These figures have been corrected for the invisible decay modes of the  $K^0$ , and for the different size of the measured sample. There is a factor of 0.56 between the fiducial volume and fraction of experiment analysed, for reactions (1) and (2).



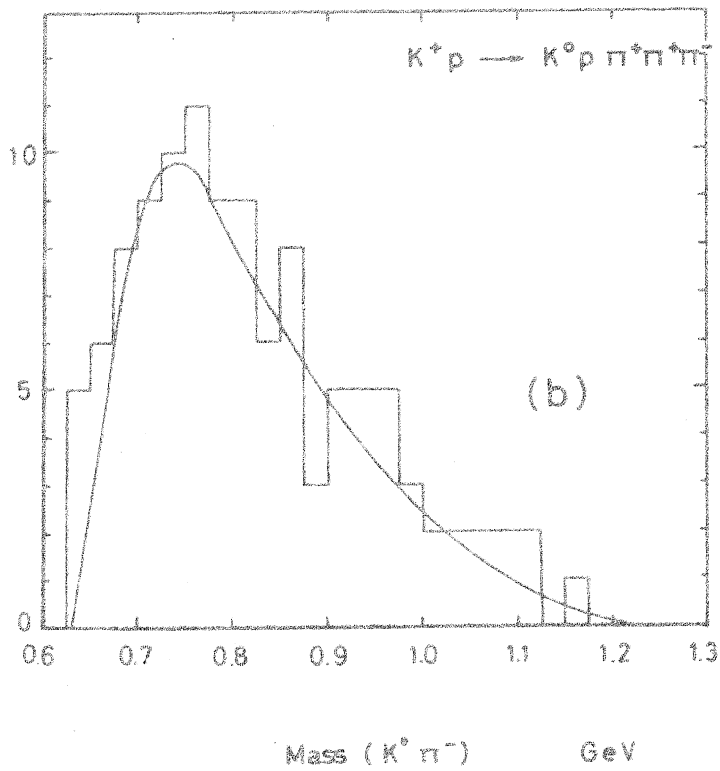
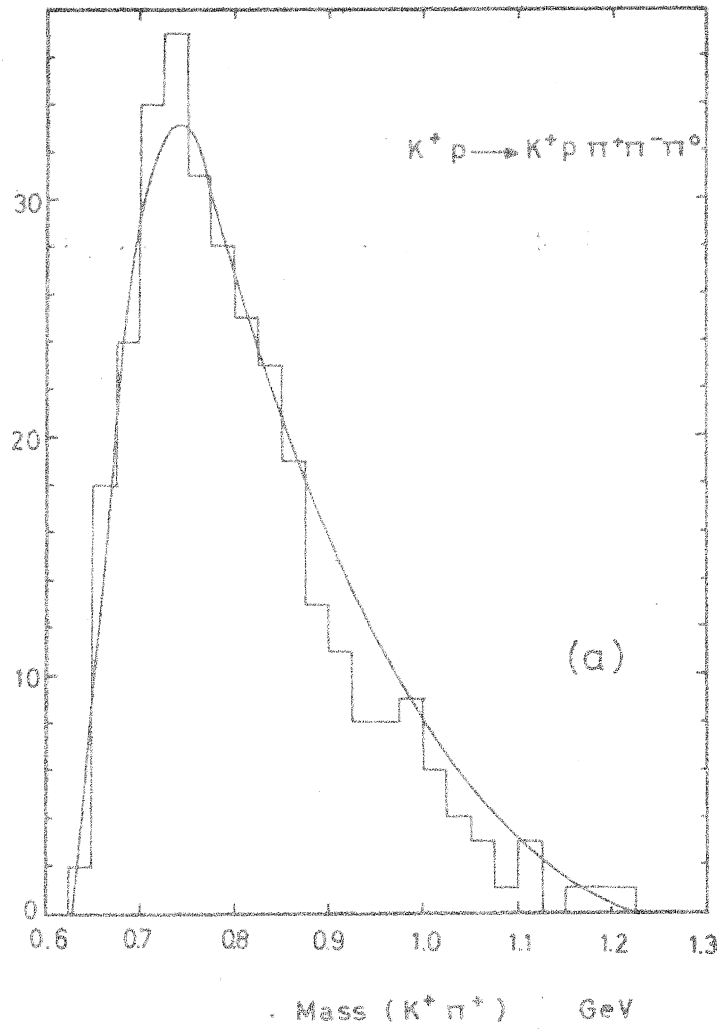




2



NUMBER OF EVENTS / 25 MeV



4

